1982ApJ...255..510L

THE ASTROPHYSICAL JOURNAL, 255:510–523, 1982 April 15
© 1982. The American Astronomical Society. All rights reserved. Printed in U.S.A.

INFRARED EMISSION LINE STUDIES OF THE STRUCTURE AND EXCITATION OF H II REGIONS

J. H. LACY
Division of Physics, Mathematics, and Astronomy, California Institute of Technology

S. C. BECK
Department of Physics, University of California, Berkeley

AND

T. R. GEBALLE
Mount Wilson and Las Campanas Observatories, Carnegie Institution of Washington
Received 1981 July 10; accepted 1981 September 29

ABSTRACT

Maps of five H II regions in one or more of the infrared fine-structure lines of Ne II (12.8 μm), Ar III (9.0 μm), and S IV (10.5 μm) have been obtained with angular resolutions ranging from 4″ to 7″. The observations are used to discuss the morphology and excitation of these nebulae. Considerable diversity is found in the structures of the nebulae, probably resulting from differences in their ages and the circumstances of their formation. In all cases, more ionizing luminosity than would be provided by a single dominant ionizing star appears to be required, although uncertainties in the model nebulae make this conclusion uncertain.

Subject headings: infrared: spectra — nebulae: H II regions

I. INTRODUCTION

Infrared emission lines from gaseous nebulae have been the subject of considerable interest in recent years. They can be used to study distant and young regions which are often obscured by dust, and they carry important information about the density, ionization state, and elemental abundances in H II regions. The most extensively studied infrared lines are in the 8–13 μm region, which is accessible to ground-based telescopes. In particular, the 9.0 μm Ar III, 10.5 μm S IV, and 12.8 μm Ne II fine-structure lines have now been detected in a large number of H II regions and planetary nebulae (Beck *et al.* 1982; Lacy 1980, and references therein).

This paper describes the results of a program of mapping the infrared fine-structure line emission from H II regions. These observations differ from previous ones in that they cover extended areas of the sky (typically more than $1' \times 1'$) with high angular resolution (4″–7″). At the distances of the galactic H II regions discussed here, this range of beam sizes corresponds to dimensions of 0.07–0.3 pc.

In this paper we first describe how the observations were made (§ II). The procedure used to derive the source characteristics from the observed line fluxes is described in § III, and the uncertainties are discussed in § IV. Conclusions about the individual nebulae are presented in § V. These conclusions are summarized, and similarities and differences among the nebulae are discussed in § VI.

II. OBSERVATIONS

Maps were made of three southern H II regions, NGC 3576 (RCW 57 or G291.3−0.7), NGC 3603 (RCW 57 II or G291.6−0.5), and G298.2−0.3, in all three ionic fine-structure lines in the 10 μm atmospheric window. Two northern sources, W3 and G29.9+0.0, were mapped in Ne II and observed at selected positions in Ar III. In addition, maps of G333.6−0.2 in all three lines are reported by Geballe *et al.* (1981), and observations of M17 and G0.5−0.1 will be reported in a later paper. Throughout this paper optical source names are used when such names exist, although in most cases the infrared sources lie in obscured regions offset from the visible nebulae.

The southern objects, NGC 3576, NGC 3603, and G298.2, were observed with the 2.5 m du Pont telescope at Las Campanas Observatory, Chile. W3 and G29.9 were observed with the 3 m Shane telescope at Lick Observatory. Information regarding the sources and observations is given in Table 1.

The observations were made with a liquid nitrogen cooled Fabry-Perot interferometer in tandem with a liquid helium cooled grating monochromator (Lacy 1979). The instrument was used both as a scanning spectrometer, to observe line profiles, and as a monochromator, to allow mapping by scanning the telescope. The spectral resolution was 0.07–0.35 cm^{-1} or 30–100 km s^{-1} (Lorentzian FWHM) which is sufficiently high that subtraction of continuum emission from the maps was not necessary.

© American Astronomical Society • Provided by the NASA Astrophysics Data System

1982ApJ...255..510L

TABLE 1

OBSERVATIONAL AND SOURCE PARAMETERS

Source	Line	Date	θ_{FWHM} (″)	$\Delta\delta$ (″)	$\Delta\alpha$ (s)	$\Delta\nu_{FWHM}$ (cm^{-1})	R_s (kpc)	T_e (K)	A_v (mag)	$A_{9.7}$ (mag)
W3A	...	...	...	...	...	...	2.4[a]	7800[b]	16[c]	2.2[d]
($2^h 22^m 54^s$	Ne II	1979 Sep	6	6	0.2	0.13	...	...	0.59	0.64
+61° 53′)	Ar III	1977 Sep	6	...	...	...	...	...	1.60	1.73
W3B	...	...	...	...	...	...	...	9500[b]	46[c]	3.3[d]
	Ne II	1977 Sep	6	6	0.2	0.13	...	...	1.70	0.96
	Ar III	1977 Sep	6	...	...	...	...	...	4.60	2.60
NGC 3576	...	...	...	...	...	...	3.6[e]	7700[e]	15[f]	3.8[f]
($11^h 09^m 47^s$	Ne II	1978 Apr	4	3	0.3	0.20	...	...	0.56	1.11
−61° 02′)	Ne II	1978 Feb	7	4	0.5	0.067	...	...	0.56	1.11
	Ar III	1978 May	7	4	0.3	0.32	...	...	1.50	2.99
	S IV	1978 May	7	4	0.2	0.25	...	...	1.55	3.08
NGC 3603	...	...	...	...	...	...	8.2[e]	6900[e]	4[g]	1.6[f]
($11^h 12^m 59^s$	Ne II	1979 Mar	7	6	1.0	0.08	...	...	0.15	0.47
−61° 00′)	S IV	1979 May	7	6	0.5	0.22	...	...	0.41	1.26
G298.2−0.3	...	...	...	...	...	...	11.[e]	8100[e]	14[f]	1.6[f]
($12^h 07^m 21^s$	Ne II	1978 Apr	4	3	0.4	0.20	...	...	0.78	0.47
−62° 33′)	Ar III	1978 May	7	4	0.2	0.32	...	...	2.10	1.22
	S IV	1978 May	7	4	0.2	0.25	...	...	2.16	1.26
G29.9+0.0	...	...	...	...	...	...	7.1[h]	8000[h]	$\gtrsim$15[i]	2.4[i]
($18^h 43^m 30^s$	Ne II	1979 Sep	6	6	0.3	0.13	...	...	$\gtrsim$0.56	0.70
−3° 43′)										

NOTE.—θ_{FWHM}: aperture size. $\Delta\delta$: spacing between scans. $\Delta\alpha$: bin size. $\Delta\nu_{FWHM}$: spectral resolution. R_s: distance from Sun. T_e: electron temperature. A_v: visual extinction derived from optical or near-infrared measurements and corresponding extinctions at fine-structure line wavelengths. $A_{9.7}$: 9.7 μm extinction derived by Gillett *et al.* 1975 case II procedure.

[a] Reifenstein *et al.* 1970.
[b] Thum *et al.* 1980.
[c] Wynn-Williams, Becklin, and Neugebauer 1972.
[d] Lester 1979.
[e] Wilson *et al.* 1970.
[f] Persson, Frogel, and Aaronson 1976.
[g] Frogel, Persson, and Aaronson 1977.
[h] Rohlfs 1974.
[i] Soifer and Pipher 1975.

Spectral scans were made at several positions within each source to determine the central frequencies and widths of the emission lines. Lorentzian fits to these scans were used to determine the ratios of the integrated line intensities to the signals measured at the wavelengths at which the maps were made. In most cases the variation in source line width and central frequency across the nebulae was small compared to the instrumental line width, so that the ratio of line intensity to measured signal is constant for each nebula. However, Ne II was observed in NGC 3576, NGC 3603, and G29.9 with relatively high spectral resolution, and we cannot rule out the possibility that variations in the source line profile cause distortions in these maps.

The mapping was done by repetitively scanning the telescope in right ascension while chopping in right ascension between the source and blank sky. The beam throw varied from 2′ to 4′, and the telescope was usually scanned a distance of two chopper throws. Any instrumental offset signal was then removed by subtracting the second half of a scan from the first, a procedure equivalent to beam switching when observing a single source. Scans were separated in declination by somewhat less than the beam width. The data were binned in right ascension to create a rectangular grid from which the maps were constructed. Scan separations and bin sizes are given in Table 1. Positions were referenced to guide stars whose coordinates were measured by offsetting from nearby SAO stars. Relative positional uncertainties within a map are 1″ rms. Maps in different ionic lines, which were in some cases made in different years, have additional relative positional uncertainties of up to 2″.

© American Astronomical Society • Provided by the NASA Astrophysics Data System

1982ApJ...255..510L

The intensity calibration was obtained by chopping between an ambient temperature blackbody and the sky and is accurate to $\pm 20\%$, except in the high resolution Ne II maps mentioned above where uncertainties in the line widths and frequencies cause possible errors which are perhaps twice as great. In NGC 3576, where diffuse nebulosity is seen to the east of the area mapped, there is evidence for contamination by infrared line emission in the reference beam. The resulting underestimate of the line fluxes should occur for all of the lines mapped, and so its effect on the line flux ratios should tend to cancel. The radio free-free fluxes used for comparison with the infrared fluxes have also been appropriately decreased in this case. The relative intensities at different positions within a map should be more accurate than the absolute intensity calibration. The uncertainties in relative intensities are due largely to guiding errors in declination which could allow small sources to fall between scans. Relative uncertainties are typically $\pm 10\%$ for point sources and $\pm 5\%$ for extended sources.

III. ANALYSIS

In principle, sufficient information can be obtained from infrared and radio observations of a visually obscured H II region to determine its excitation, or ionization state, the degree of enrichment of heavy elements, and the motions of the ionized gas. In particular, observations of the fine structure lines of S III (18.7 μm), S IV (10.5 μm), Ar II (7.0 μm), and Ar III (9.0 μm), when compared with radio or infrared observations of ionized hydrogen, would allow a determination of S/H and Ar/H as well as the excitation in a nebula. In addition, measurements of line profiles of any of the infrared lines provide information on gas motions. Unfortunately Ar II and S III fall in regions of the spectrum that are very difficult to observe except from airplane altitudes, so that detailed mapping of these lines is not at present practical. High angular resolution observations of hydrogen recombination line or free-free continuum emission are also not available for most of the objects discussed here, particularly those south of $-30°$. Consequently, we use the observations of Ne II (12.8 μm), Ar III (9.0 μm), and S IV (10.5 μm) presented in this paper primarily to discuss the spatial distribution of the ionized gas and, by assuming that the abundances of neon, sulfur, and argon are solar, to derive qualitative information about the excitation of the nebulae studied.

The intensity of the line observed from the fine-structure splitting of the ^2P ground state of a p^1 or p^5 ion, such as Ne^+ and S^{+3}, may be expressed as

$$I_{fs}(\text{ergs s}^{-1}\text{ cm}^{-2}\text{ sr}^{-1}) = 4.2\times 10^{-7} K_i \gamma_i \left(\frac{10^4\text{ K}}{T_e}\right)^{1/2} \times e^{-hc/\lambda k T_e} \int \frac{n_c}{n_e + n_c} n_e n_p \, dl \,(\text{cm}^{-6}\text{ pc}) \quad (1)$$

(Petrosian 1970). Here γ_i is the number abundance of the ion ($\gamma_{H^+} = 10^4$), K_i a line strength factor, and n_c the critical density for collisional thermalization of the fine-structure levels. The intensity of the $^3P_1 - {}^3P_2$ transition of Ar III has a more complicated density dependence but at low densities is adequately described by equation (1). Since $n_c = 3.6\times 10^5$ cm^{-3} for Ne II, $\sim 3\times 10^5$ cm^{-3} for Ar III, and 7.1×10^4 cm^{-3} for S IV, and the density in the H II regions studied here is $\sim 10^3 - 10^4$ cm^{-3}, we assume $n_c/(n_e + n_c) = 1$. The electron kinetic temperature, T_e, is taken from radio work. The line strength factors are $K_i = (\Omega_{21}/g_1)$ (10 μm$/\lambda$) $= 0.071$ for Ne II, 0.62 for Ar III, and 0.81 for S IV, where the collision strengths, Ω, are those of Seaton (1975) for Ne II, Kreuger and Czyzak (1970) for Ar III, and Brocklehurst (1972) for S IV, and $g_1 = 2J_1 + 1$ is the degeneracy of the lower level.

At low densities, the relative intensities of fine-structure lines, calculated from equation (1), depend only on ratios of atomic constants and ionic abundances. The fractional ionic abundances, $x(Z^{+n}) = \gamma_{Z^{+n}}/\gamma_Z$, depend on the spectral distribution and luminosity of the ionizing radiation and the gas density. If the ionizing spectrum is not altered by absorption by dust and the ionizing stars are on the main sequence, the spectral distribution and luminosity of the ionizing radiation are determined by the spectral types of the ionizing stars. Consequently, for an assumed gas density and assumed relative elemental abundances, the intensity ratio of two ionic fine-structure lines can be used to estimate the stellar spectral types.

We assume solar elemental abundances, the ratios of which are likely to remain relatively constant even if the gas is enriched in heavy elements. The assumed cosmic abundances, $\gamma_{Ne} = 0.83$, $\gamma_{Ar} = 0.063$, and $\gamma_S = 0.16$, with $\gamma_H = 10^4$, are taken from Allen (1973). We obtain $x(Z^{+n})$ from Balick and Sneden's (1976) model nebulae, with $n_H = 10^3$, using $Z = Z_\odot$, $\log g = 4$ stellar atmosphere models. The actual densities of the nebulae and the errors introduced by assuming $n_H = 10^3$ cm^{-3} are discussed in § V below. Since Balick and Sneden do not include argon ionic abundances, we assume, based on the similarity of ionization potentials, that $x(Ar^{+2})$ is the lesser of $x(N^{+2})$ and $x(Ne^+)$. Note, however, that this procedure does not allow $x(Ar^{+2}) > x(Ne^+)$, in contradiction to the work of Köppen (1978, 1980) and in contradiction to some of the observations presented below. The neon abundance used by Balick and Sneden is ~ 4 times ours, but as they point out, changes in γ_{Ne} should not change the nebular ionization structures or $x(Ne^+)$.

For the purpose of discussing the variation in excitation across the H II regions, each nebula has been divided into from one to seven sources. The fine-structure line fluxes from each source were obtained by integrating over the line intensity maps. The measured fluxes

© American Astronomical Society • Provided by the NASA Astrophysics Data System

1982ApJ...255..510L

TABLE 2

LINE FLUXES AND EMISSION MEASURES

SOURCE	F (10^{-10} ergs s^{-1} cm^{-2}) Ne II	Ar III	S IV	F (Jy) H II	F_c (10^{-10} ergs s^{-1} cm^{-2}) Ne II	Ar III	S IV	E_i (cm^{-6} pc^3) Ne^+	Ar^{+2}	S^{+3}	H^+
W3(A)	16.92	2.18	...	33.00[a]	29.06	9.52	...	56.5	2.3	...	1.8e+06
(B)......	3.48	0.03	...	10.00	16.50	2.28	...	34.5	0.6	...	5.9e+05
N3576	46.13	12.56	20.12	38.00[b]	76.60	49.99	83.86	333.7	27.3	31.8	4.1e+06
1	9.79	3.55	8.04	...	16.25	14.13	33.49	70.8	7.7	12.7	...
2	12.10	3.76	4.92	...	20.10	14.98	20.49	87.6	8.2	7.8	...
3	8.82	2.24	1.98	...	14.65	8.94	8.25	63.8	4.9	3.1	...
4	3.71	0.24	−0.04	...	6.17	0.94	−0.18	26.9	0.5	−0.1	...
5	5.36	0.79	0.99	...	8.90	3.14	4.12	38.8	1.7	1.6	...
6	3.85	1.18	1.86	...	6.39	4.69	7.86	27.8	2.6	3.0	...
7	2.82	0.80	2.17	...	4.68	3.17	9.05	20.4	1.7	3.4	...
N3603	16.13	...	41.43	21.00[c]	18.47	...	60.62	401.9	...	115.3	1.1e+07
E	11.59	...	29.66	...	13.27	...	43.39	288.8	...	82.6	...
W	4.54	...	11.77	...	5.20	...	17.23	113.1	...	32.8	...
G298.2 ...	6.31	3.62	12.68	31.00[d]	10.13	13.13	48.03	499.2	81.0	205.9	4.3e+07
E	3.83	2.24	8.22	...	6.14	8.12	31.16	302.8	50.1	133.6	...
W	2.48	1.38	4.45	...	3.98	5.01	16.87	196.4	30.9	72.3	...
G29.9	8.36	0.84	0.29	2.90[d]	13.89	3.34	1.21	238.6	7.2	1.8	$a.b \times 10^c$

[a] Harris and Wynn-Williams 1976.
[b] Retallack and Goss 1975.
[c] Shaver and Goss 1970.
[d] Felli, Tofani, and D'Addario 1974.

and the fluxes corrected for interstellar extinction are listed in Table 2. Also listed are integrated ionic emission measures, $\int E_i = \int n_i n_e \, dV$, derived from the extinction corrected fluxes using equation (1) integrated over solid angle, and integrated proton emission measures, derived from radio free-free observations. In cases where spectral scans rather than maps were made of an ion, the flux from a source was estimated by assuming the ion to have the same distribution as another which was mapped.

Fractional ionic abundance ratios, $x(S^{+3})/x(Ne^+)$ and $x(Ar^{+2})/x(Ne^+)$ were obtained from emission measure ratios and are listed in Table 3. The effective temperature and spectral type of a main-sequence star which would produce these abundance ratios were estimated from Balick and Sneden's (1976) models. The integrated proton emission measure was then calculated from $\int E_{Ne+}$ by $\int E_{H^+} = \int E_{Ne^+}/[x(Ne^+)\gamma_{Ne}]$, using $x(Ne^+)$ from Balick and Sneden. The Lyman continuum luminosity required to ionize the gas was calculated from $N_{Lyc}(fs) = \alpha_B \int E_{H^+}$, where α_B is the case B effective recombination coefficient for hydrogen (Osterbrock 1974). Also listed in Table 3 is the Lyman continuum luminosity provided by a main-sequence star of the derived spectral type, N_{Lyc}(MS), the Lyman continuum luminosity derived from radio free-free observations, N_{Lyc}(ff), and the Lyman α luminosity which would account for the 1–20 μm luminosity of each nebula, $N_{Ly\alpha}$(IR). The estimates of luminosity are used below to discuss the number of ionizing stars and the amount of nonionizing radiation.

IV. UNCERTAINTIES

In determining the spectral types of the stars which ionize the observed nebulae, uncertainties in the measured fluxes are relatively unimportant sources of error. The most significant sources of error are uncertainties in (1) the elemental abundances of neon, sulfur, and argon, (2) the extinctions to the nebulae, (3) the electron densities in the nebulae, and (4) other parameters of the models. The first two of these uncertainties affect the derivation of the fractional ionic abundance ratios from the line flux ratios. The second two affect the determination of the stellar spectral types from the ionic abundance ratios.

Variations or errors in the relative abundances of the observed elements would have quite different effects on the derived parameters than would variations in all three elements together relative to hydrogen. Equal changes of γ_{Ne}, γ_{Ar}, and γ_S, as would result, e.g., from a galactic abundance gradient, would affect $\int E_p$ and the derived number of ionizing stars. In contrast, a change in γ_{Ne}/γ_S or γ_{Ne}/γ_{Ar} would affect, proportionately, the derived values of $x(S^{+3})/x(Ne^+)$ or $x(Ar^{+2})/x(Ne^+)$, from which T_{eff} is derived. The assumed abundances of neon

© American Astronomical Society • Provided by the NASA Astrophysics Data System

1982ApJ...255..510L

TABLE 3
IONIC ABUNDANCE RATIOS AND STELLAR CHARACTERISTICS

Source	$\frac{x(S^{+3})}{x(Ne^{+})}$	$\frac{x(Ar^{+2})}{x(Ne^{+})}$	T_{eff} (10^3 K)	Spectral Type	$\int E_p$	N_{Lyc}(T) (10^{48} s^{-1})	N_{Lyc}(fs) (10^{48} s^{-1})	N_{Lyc}(ff) (10^{48} s^{-1})	$N_{Ly\alpha}$(IRC) (10^{48} s^{-1})
W3(A).......	...	0.54	36.1	O8.0	$7.2e+05$	3.2	5.5	13.8	30.5[a]
(B)........	...	0.23	33.9	O9.0	$4.3e+05$	1.5	3.3	4.5	5.9
N3576.......	0.49	1.08	37.3	O7.5	$4.3e+06$	4.8	33.2	31.4	186.6[b]
1	0.93	1.44	39.2	O7.0	$1.0e+06$	8.4	7.6	...	...
2	0.46	1.23	37.3	O7.5	$1.1e+06$	4.8	8.7	...	...
3	0.25	1.01	36.4	O8.0	$8.1e+05$	3.6	6.2	...	...
4	0.00	0.25	33.9	O9.0	$3.3e+05$	1.5	2.6	...	...
5	0.21	0.58	36.1	O8.0	$4.9e+05$	3.2	3.7	...	...
6	0.56	1.21	37.7	O7.5	$3.7e+05$	5.3	2.8	...	...
7	0.87	1.12	38.9	O7.0	$2.8e+05$	7.7	2.2	...	...
N3603.......	1.49	...	42.0	O6.0	$7.5e+06$	17.8	57.0	86.8	1482.8[b]
E	1.48	...	42.0	O6.0	$5.4e+06$	17.8	41.0	...	...
W	1.50	...	42.0	O6.0	2.1e+06	17.8	16.0	...	...
G298.2	2.14	2.14	44.2	O5.5	$1.4e+07$	29.8	108.0	329.1	589.8[b]
E	2.29	2.18	44.5	O5.5	$9.3e+06$	32.0	70.8	...	...
W	1.91	2.08	43.6	O5.5	$4.8e+06$	25.9	36.9	...	...
G29.9	0.04	0.40	33.9	O9.0	$a.b \times 10^c$	1.5	22.7	11.6	94.0[c]

[a] Hackwell *et al.* 1978.
[b] Frogel, Persson, and Aaronson 1977.
[c] Soifer and Pipher 1975.

and sulfur are probably reasonably accurate for nebulae in the solar neighborhood. The argon abundance is much less well known and could be in error by as much as a factor of 2 (see Beck *et al.* 1981). Because of this uncertainty and the lack of calculated models which include argon, the Ar III results are used to derive stellar temperatures only for W3 for which S IV observations were not made.

Extinction at infrared wavelengths, although much smaller than in the optical region, is difficult to determine and can be significant. Published extinction values, derived by two different methods, are listed in Table 1. The figures in the column labeled A_v were derived from optical or near-infrared measurements, most often from measurements of 1.65–2.2 μm colors, by assuming that the emission at both wavelengths is due to free-free and free-bound transitions in the ionized gas. The figures in the column labeled $A_{9.7}$ were derived by the Gillett *et al.* (1975) case II 10 μm continuum fitting procedure. The extinction figures at the fine-structure line wavelengths, derived assuming the extinction curve of Becklin *et al.* (1978): $A_{9.0}=10.0, A_{9.7}=12.7$, $A_{10.5}=10.3$, and $A_{12.8}=3.7$ for $A_v=100$ mag, are given below A_v and $A_{9.7}$. Sources for A_v and $A_{9.7}$ are given in the footnotes to Table 1. The extinctions derived from A_v are used for the calculations in Tables 2 and 3.

In the worst case, W3B, the two extinction determinations differ by 2 mag in $A_{9.0}$ and 1.5 mag in $E_{9.0-12.8}$. Fortunately, the effects of an error in the extinction tend to cancel in the conclusions about the number of ionizing stars. Because the extinction increases from Ne III to Ar II to S IV, an underestimate of the extinction would cause an underestimate of the derived stellar temperatures and hence the ionizing flux of the stars as well as the required ionizing fluxes. Effects of possible errors in the extinctions are discussed in § V for the nebulae in which such errors are likely.

The excitation of a radiation bounded nebula of uniform density depends not only on the spectral types of the ionizing stars, but also on the product of the ionizing luminosity and the nebular density (see Köppen 1978). Values of $x(S^{+3})/x(Ne^{+})$ for different values of T_{eff} and n_e were calculated from models of three authors and are plotted in Figure 1. For a fixed T_{eff}, $x(S^{+3})/x(Ne^{+})$ decreases with increasing n_e, although the models disagree on the exact nature of the dependance. The rms electron densities in the cores of the observed nebulae range from the assumed value, 10^3 cm^{-3}, up to $\sim 10^4$ cm^{-3}.

Another source of uncertainty is the large disagreement in calculated fractional ionic abundances between published model nebulae, as is seen in Figure 1.

© American Astronomical Society • Provided by the NASA Astrophysics Data System

1982ApJ...255..510L

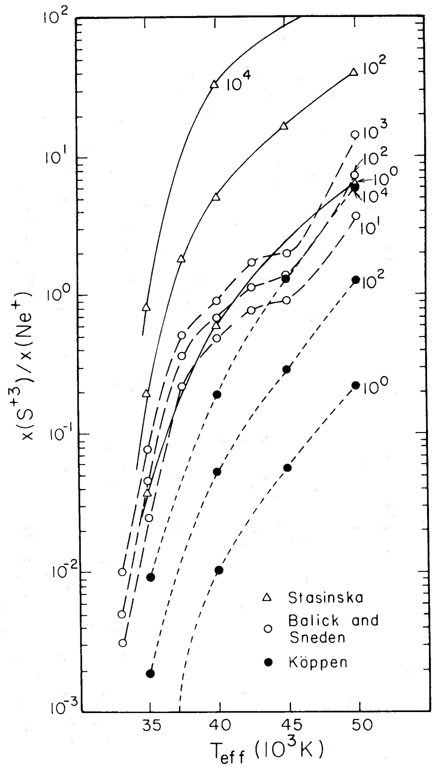

FIG. 1.—Fractional ionic abundance ratio, $x(S^{+3})/x(Ne^{+})$, vs. stellar temperature, T_{eff}. Three models, labeled by n_e (cm^{-3}), are shown for each of three different authors.

The models of Köppen (private communication) and Stasinska (1978) differ by as much as a factor of 100. R. H. Rubin (private communication) has calculated several model nebulae with the parameters and stellar spectra used by Köppen and Stasinska. He finds that the differences in the calculations are primarily due to differences in the stellar spectra. Köppen used spectra from Kurucz, Peytreman, and Avrett (1974), whereas Stasinska used NLTE stellar spectra from Mihalas (1972).

Different choices of stellar model spectra or nebular gas density result primarily in vertical shifts of the curves in Figure 1. A vertical shift of a factor of 10 would change the derived value of T_{eff} by ~2500 at 35,000 K and by ~8000 at 45,000 K. In the discussion of the individual sources (§ V), we assume that the models of Balick and Sneden (1976) with $n_e = 10^3$ cm^{-3} accurately represent the observed nebulae. Ways in which the conclusions depend on the choice of models are discussed in § VI.

Other factors also affect the degree of ionization of the model nebulae. For example, the presence of dense optically thin clumps within a nebula lowers its average excitation (Köppen 1979). Several of the nebulae show obvious large scale clumping, but no adequate models with which to compare this structure have been published.

V. RESULTS

a) *W3* (*main*)

W3 (Fig. 2) is the most studied of the objects discussed in this paper. It has been mapped in the radio continuum by Harris and Wynn-Williams (1976) and Colley (1980). Harris and Wynn-Williams (1976) and Wynn-Williams, Becklin, and Neugebauer (1972) suggest that W3A is an ionization bounded H II region ionized by two highly obscured stars, IRS 2 and IRS 2a (Beetz, Elsässer, and Weinberger 1974). The radio continuum luminosity of W3A and the infrared fluxes of IRS 2 and IRS 2a are consistent with IRS 2 being an O5–O6 V star and IRS 2a being a ~O9 V star.

Hackwell *et al.* (1978) have mapped the mid-infrared continuum emission from W3. They conclude that the dust within W3A is heated by Lyα emission from the ionizated gas. They also find a variable extinction across W3A, with $\tau_{9.7} = 2.0$ toward the center, rising to $\tau_{9.7} = 4.0$ at the rim. Herter *et al.* (1980) and Lacasse *et al.* (1980) have studied the spatial distribution of Ne II, Ar II, Ar III, and S IV fine-structure line emission from W3A. They prefer a model in which the H II region is ionized by an O5 V star whose ionizing spectrum is softened by selective absorption by dust mixed with the ionized gas.

The spatial distribution of Ne II emission from W3 is shown in Figure 2, along with the distribution of 5 GHz free-free emission from Harris and Wynn-Williams (1976). With the exception of the somewhat lower spatial resolution of the Ne II map and the larger extinction toward W3B than W3A, the two maps are nearly identical. This similarity casts some doubt on Hackwell *et al.*'s (1978) conclusion that the extinction varies across W3A, although the predicted variation is only ~0.5 mag at Ne II and peaking of the Ne II emission toward the rim would compensate for an extinction variation. The small source in the Ne II map labeled 5 is IRS 5, which is not believed to be associated with ionized gas. The 12.8 μm flux at this source is consistent with Willner's (1977) measurement of the continuum flux at this wavelength. This is the only case in which a continuum source is thought to contribute significantly to an emission line map in this paper.

W3A and W3B appear to be ionization bounded H II regions, still surrounded by the molecular cloud out of which they formed. Both show shell structure, at least in the higher resolution radio map. In contrast to other sources discussed in this paper, this structure is essentially that expected from an H II region in a uniform molecular cloud. The observed shell structure can be explained by radiation pressure or a stellar wind from the ionizing stars (Harris and Wynn-Williams 1976).

© American Astronomical Society • Provided by the NASA Astrophysics Data System

1982ApJ...255..510L

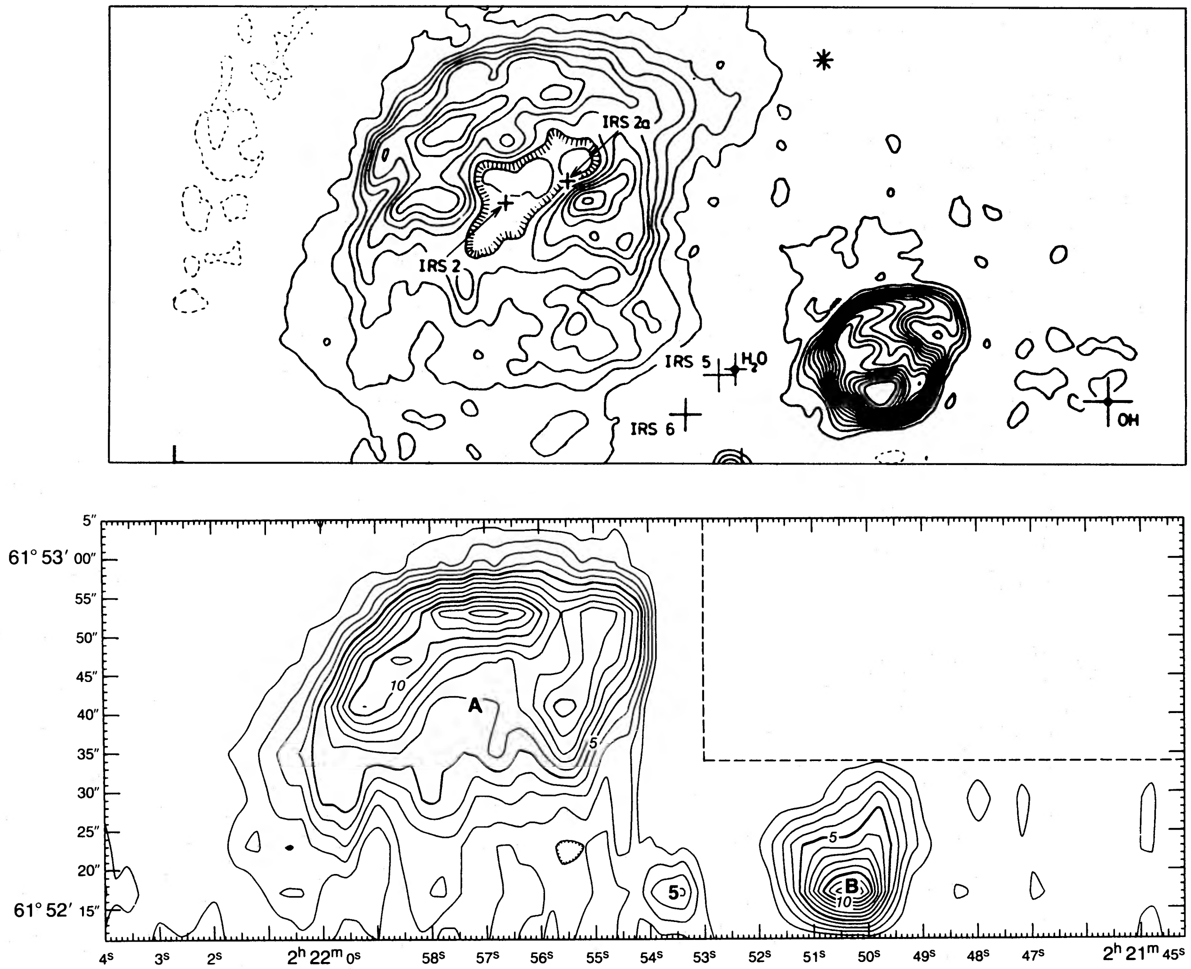

FIG. 2.—Ne II line map (*lower*) and 5 GHz continuum map (*upper*, from Harris and Wynn-Williams 1976) of W3. Ne II contour interval is 7.4×10^{-3} ergs s^{-1} cm^{-2} sr^{-1}. The area within the dotted line was not mapped.

Since Ar III and S IV were not mapped in W3, its excitation was determined from comparison of the Ne II and 5 GHz maps with Ar III spectral scans. The Ar III/Ne II intensity ratio indicates that W3A is ionized by a star of spectral type O8 and W3B by an O9 star, assuming the extinction figures of Wynn-Williams, Becklin, and Neugebauer (1972). However, main-sequence stars of these spectral types would provide only ~ one-third the ionizing luminosities required to explain the Ne II fluxes, N_{Lyc}(fs) in Table 3, and ~one-third those required by the radio observations, N_{Lyc}(ff). The factor of ~2 discrepancy between the luminosity derived from Ne II and that from the radio free-free suggests that the extinction has been underestimated. If A_v is increased by 10 mag toward W3A and W3B, the derived spectral types become O7 and O8.5 and N_{Lyc}(fs) $= N_{\mathrm{Lyc}}$(ff). Main-sequence stars of these spectral types would account for ~one-half of N_{Lyc}. The remaining discrepancy and the discrepancy with the spectral type derived for IRS 2 may indicate softening of the ionizing radiation by dust absorption, as suggested by Lacasse *et al.* (1980) or may result from inaccuracies in the models used. Because of the shell structures of W3A and B, the brightest parts of the nebulae are farther from the ionizing stars than in the modeled uniform nebulae. Consequently, they should be of lower excitation than predicted by the models.

b) *NGC 3576 = RCW 57 = G291.3 − 0.7*

The infrared and radio emission from NGC 3576 (Figs. 3 and 4 [Pl. 5]) peak in a highly obscured region to the southwest of the optical nebula. The Ne II contour map is shown in Figure 4, superposed on photograph taken through a [S II] interference filter by T. R. Gull. Little optical emission is seen from the region which is brightest in the infrared, and there is no optical evidence of the bright ridge toward the western edge of

© American Astronomical Society • Provided by the NASA Astrophysics Data System

1982ApJ...255..510L

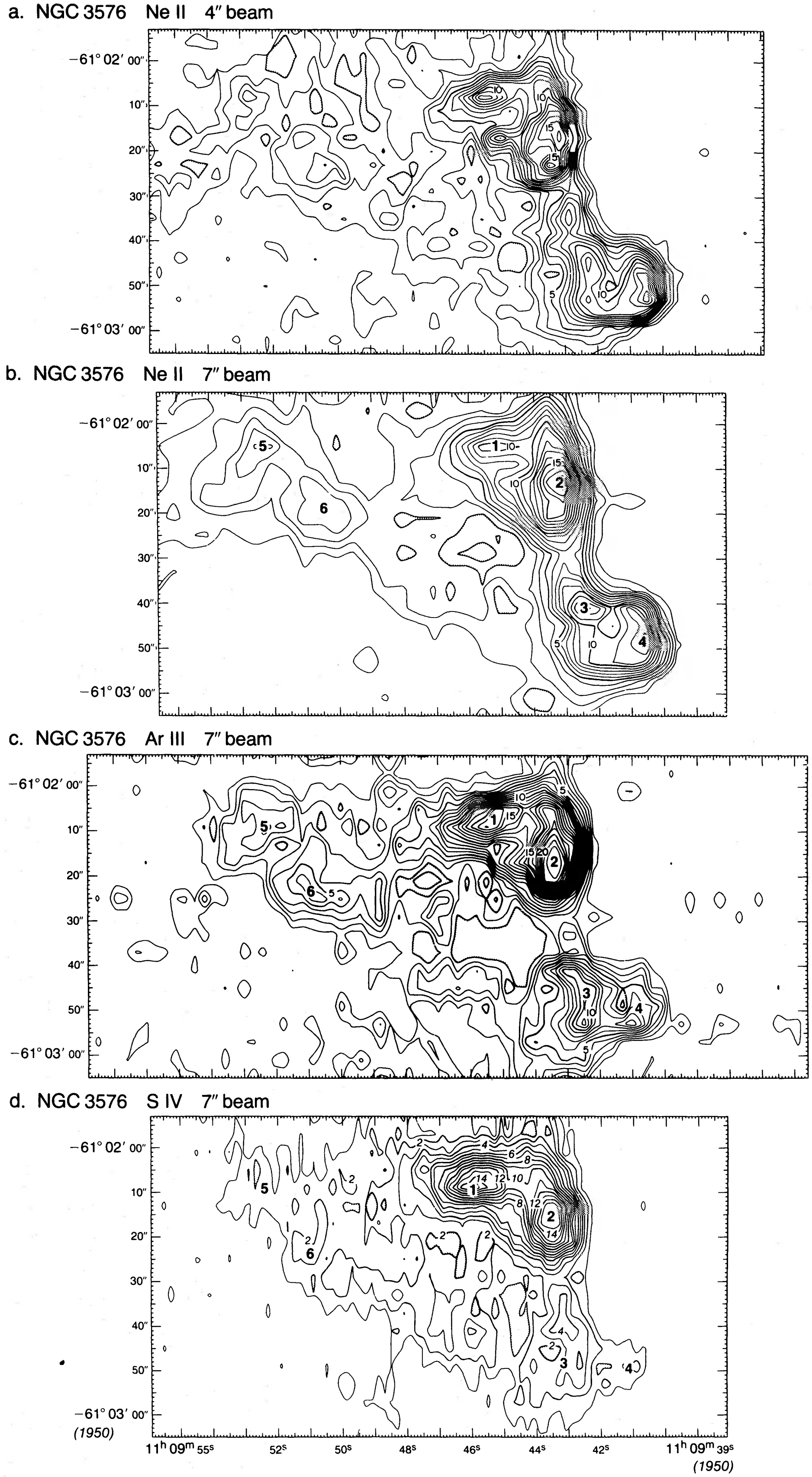

FIG. 3.—Ne II, Ar III, and S IV line maps of NGC 3576. Contour intervals are (*a*) 9×10^{-3}, (*b*) 1.0×10^{-2}, (*c*) 3.0×10^{-3}, (*d*) 7.0×10^{-3} ergs s^{-1} cm^{-2} sr^{-1}.

© American Astronomical Society • Provided by the NASA Astrophysics Data System

1982ApJ...255..510L

the fine-structure line maps. The closest correspondence is between the weaker infrared sources to the east and the southwestern edge of the optical emission. The 10 μm continuum emission from the vicinity of the radio peak in NGC 3576 was mapped by Frogel and Persson (1974) with 14."5 resolution. They observed four extended sources, IRS 2–5, and an unresolved possibly protostellar source, IRS 1. All four extended sources are seen in the infrared line maps, although each separates into at least two peaks with 7" resolution, and $\sim$16 peaks can be seen in the 4" resolution Ne II map. The free-free emission from this region has been mapped at 1.4 GHz by Retallack and Goss (1980) with a $55'' \times 49''$ beam. They observe emission coextensive with the infrared emission but do not separate the various peaks.

The structure of NGC 3576 suggests that it is an example of sequential star formation as described by Elmegreen and Lada (1977). In their model an H II region which has formed near the edge of a molecular cloud drives a shock front and an ionization front into the molecular cloud. Between the two fronts a layer of compressed gas builds up which becomes gravitationally unstable after $\sim 3 \times 10^6$ yr and forms a new generation of stars. These stars would then ionize a new H II region which expands to break out of the molecular cloud while driving a new shock and ionization front into the cloud to repeat the process. The optical nebula of NGC 3576 lies just outside of a molecular cloud, whereas the radio and infrared H II region is just inside the cloud, as would be expected if the obscured nebula formed in the layer compressed by the older optical H II region. There is some evidence that the younger region is breaking out of the molecular cloud, since the eastern extension of the infrared emission adjoins the brightest part of the optical nebula. The abrupt western edge of the infrared emission seems clearly to be an ionization front between the molecular cloud and the H II region.

We have somewhat arbitrarily (especially in light of the structure seen in the 4" Ne II map) divided the ionized gas maps into seven sources, the peaks of which are labeled in Figure 3. The observed and calculated parameters describing these sources are listed in Tables 2 and 3. The extinction corrections were taken from Frogel and Persson who give $A_v = 13.6$ mag. The figures in Table 3 indicate that typically one main-sequence star is required to ionize each source. This fact must however be fortuitous, since there is little reason to separate the sources in the way we have. The relative constancy of the Ne II/Ar III/S IV intensity ratios over the region of sources 1 and 2 and over sources 3 and 4 suggests that these two regions are each ionized by a single star or a collection of similar stars. The ionic line ratios of sources 1 and 2 indicate that one or more O7 stars ionize this gas, whereas sources 3 and 4 require a spectral type $\sim$O8.5. In each case two or three main-sequence stars of the indicated spectral type would be required to account for the ionization of the observed gas. A total of about eight O7.5 V stars could ionize the entire observed region.

Since the ionizing stars of the NGC 3576 infrared and radio nebula have not been observed, ionization by a collection of stars like that suggested here cannot be ruled out. An alternative is that two more luminous stars dominate the ionization of the nebula. They could be more luminous than main-sequence stars of their spectral type, their ionizing spectra could be softened by absorption by dust mixed with the ionizing gas, or the clumpy structure of the nebula could lower its excitation. Absorption of ionizing photons by dust is suggested by the fact that the infrared luminosity of the dust in the H II region, observed by Frogel, Persson, and Aaronson (1977), is $\sim$6 times that which would result from Lyα absorption alone. It is surprising, however, that a high excitation region is not seen surrounding each ionizing star if this is the case.

There is a great deal of structure in NGC 3576 which is apparently not due to the distribution of ionizing stars. The relatively constant Ne II/S IV intensity ratio across large areas of the maps indicates that this structure cannot be due to very nonuniform extinction and probably not to nonuniform absorption of ionizing radiation by dust. The ionized gas must, in fact, be quite clumpy. Significant clumping is seen down to the 4" beam size, which corresponds to $\sim$0.07 pc. Expansion at 10 km s^{-1} would double the size of such a clump in only $\sim$5000 yr. Although neutral condensations might replenish the clouds, allowing them to persist for longer than this, the compact H II region must be quite young compared to the $\sim 10^7$ yr lifetime of the ionizing stars.

c) *NGC 3603 = RCW 57 II = G291.6 − 0.5*

NGC 3603 (Figs. 5 and 6 [Pl. 6]) has been observed by Frogel, Persson, and Aaronson (1977) in the mid-infrared continuum, by Balick, Boeshaar, and Gull (1980) in optical emission lines, and by Retallack and Goss (1980) at 1.4 GHz. Except for differences in angular resolution, the nebula appears essentially the same at all of these wavelengths and in the infrared fine-structure lines.

Balick *et al.* point out that NGC 3603 is a relatively unobscured giant H II region with a dense core of $n_e \approx 2000$ cm^{-3} and $d \approx 7$ pc, and a faint halo of $n_e \approx 100$ cm^{-3} and $d \approx 50$ pc. The infrared maps cover the brightest part of the core. The nebula is ionized by a cluster of stars centered at $11^h12^m57^s.8$, $-60°59'16''$, on the northern edge of the region mapped.

The Ne II contour map is shown superposed on the [N II] photograph of Balick *et al.*, and the S IV map is superposed on their [O III] photograph in Figure 6. As they point out, there appears to be an evacuated bubble surrounding the star cluster. A bright rim is seen on the

© American Astronomical Society • Provided by the NASA Astrophysics Data System

1982ApJ...255..510L

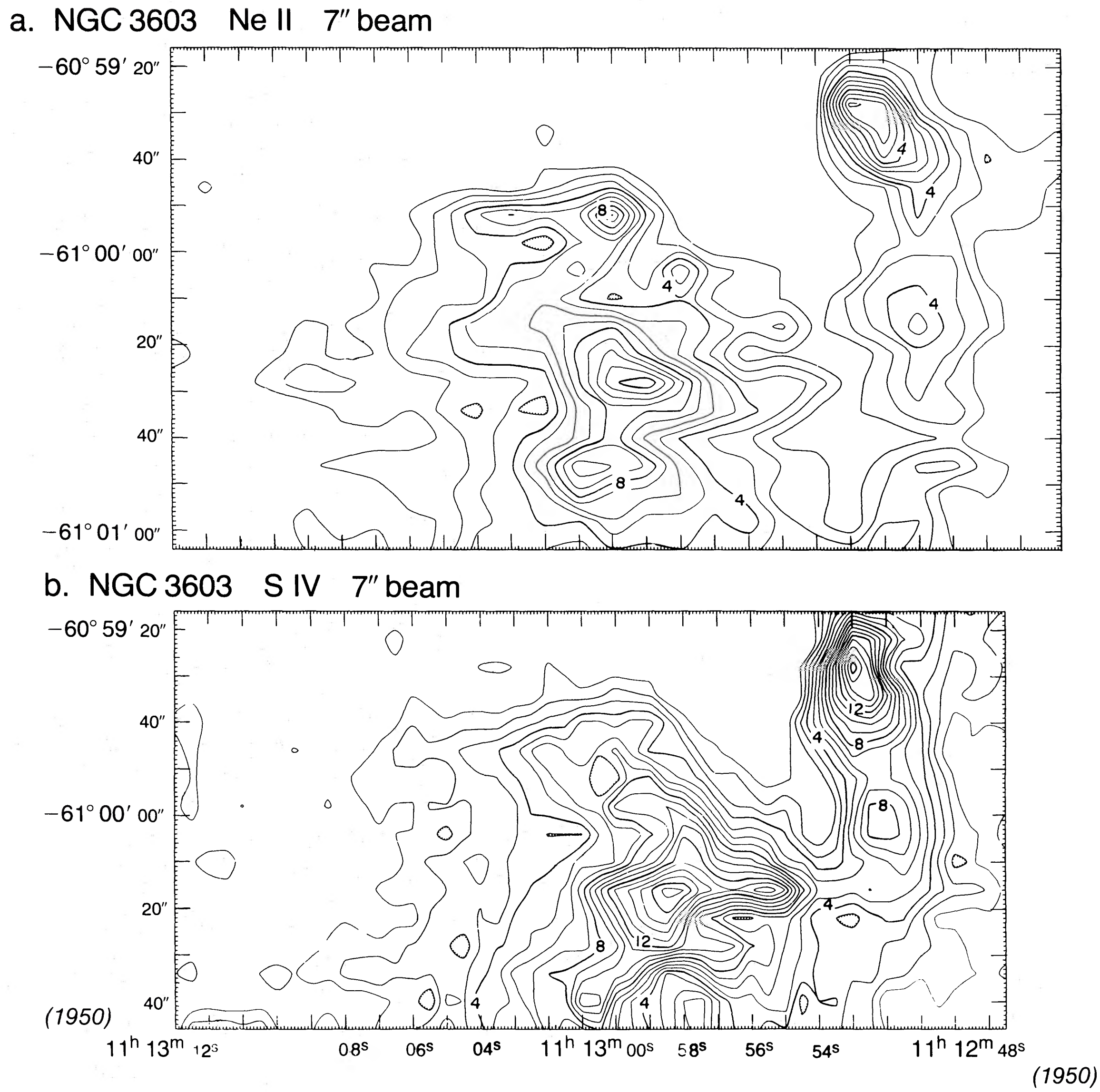

FIG. 5.—Ne II and S IV line maps of NGC 3603. Contour intervals are (*a*) 2.1×10^{-3}, (*b*) 3.6×10^{-3} ergs s^{-1} cm^{-2} sr^{-1}.

southwestern edge of the bubble in the [O III] photograph. The lack of ionized gas near the cluster is also apparent in the infrared maps, and the S IV emission peaks toward the [O III] rim, although the rim itself is not apparent. Detailed inspection of the Ne II and S IV maps reveals an offset of the S IV peaks toward the star cluster from the Ne II peaks. This displacement can also be seen between [O III] and [N II] and probably results from a softening of the ionizing radiation as it is absorbed by the gas and dust in the H II region.

The nebula is simply divided into an eastern and a western source in Tables 2 and 3. The S IV/Ne II ratio is essentially the same in both sources and indicates a spectral type of the ionizing radiation of ~O6. About four O6 V stars would provide the required ionizing luminosity. As is discussed above, the ionizing stars are probably not embedded in the ionized gas, however. The observed gas probably absorbs a small fraction of the ionizing luminosity of the star cluster. If the ionized gas is separated from the source of ionizing radiation, the nebular models used should not necessarily be applicable. Stars hotter than O6 may be present. The infrared continuum luminosity of NGC 3603 is much larger than could be explained by Lyα heating. Absorption of both ionizing and nonionizing stellar radiation by dust is probably occurring.

© American Astronomical Society • Provided by the NASA Astrophysics Data System

1982ApJ...255..510L

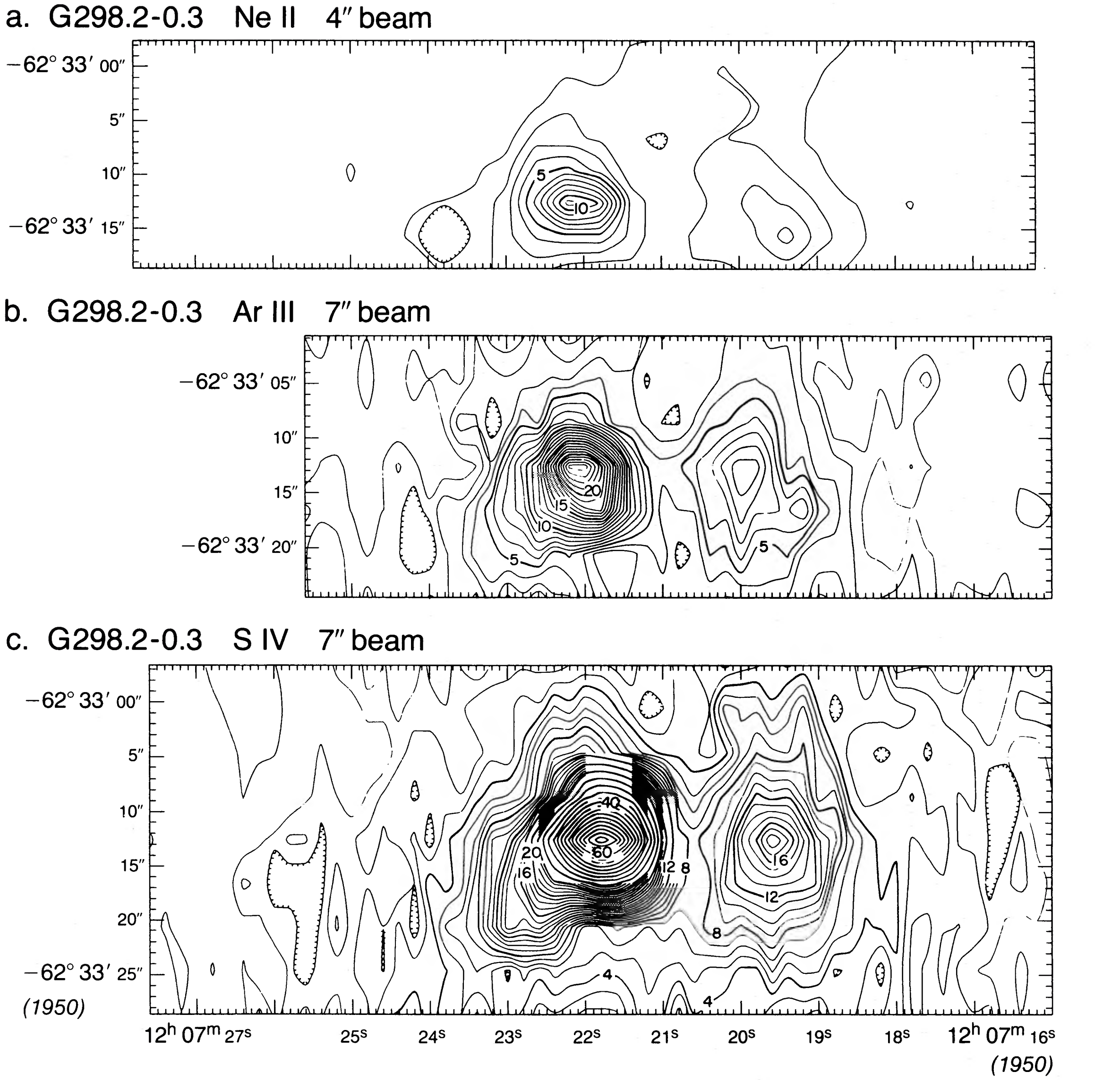

FIG. 7.—Ne II, Ar III, and S IV line maps of G298.2−0.3. Contour intervals are (*a*) 1.4×10^{-2}, (*b*) 3.1×10^{-3}, (*c*) 4.1×10^{-3} ergs s^{-1} cm^{-2} sr^{-1}.

d) *G298.2 − 0.3*

G298.2−0.3 (Fig. 7) is the most luminous known galactic H II region. It has been mapped in the infrared continuum by Frogel and Persson (1974) and has been observed in infrared emission lines by Rank *et al.* (1978). Frogel and Persson observed a single peak, coincident with the eastern peak in our maps, with a shoulder to the west. Rank *et al.* observed Ne II and S IV with a 6″ aperture centered on the eastern peak and a 14″ N-S chop. Their relative line fluxes agree acceptably with ours, although their beam takes in only $\sim 1/20$ of the emission we mapped. Three peaks can be seen in the fine-structure line maps. The eastern peak is bright in all three lines. A second peak is seen 2^{s}2 W in S IV and Ar III. A third peak, southwest of the second, is seen in Ar III and Ne II. In addition, a diffuse background is seen in all three ionic lines. The apparently simple structure of this nebula is probably a result of its 11 kpc distance (Wilson *et al.* 1970). Higher spatial resolution observations might well show considerably more detail.

G298.2−0.3 has been divided into only two regions, with the western and southwestern sources considered together. This was done because the southwestern source is much weaker than the western source and only marginally resolved from it. The presence of low excitation

© American Astronomical Society • Provided by the NASA Astrophysics Data System

1982ApJ...255..510L

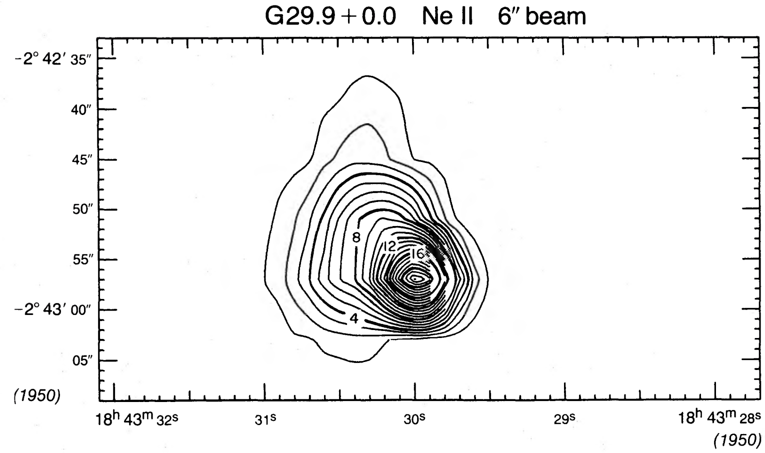

FIG. 8.—Ne II line map of G29.9+0.0. Contour interval is 1.5×10^{-2} ergs s^{-1} cm^{-2} sr^{-1}.

gas in the southwestern source suggests that it may be a separate region ionized by cooler stars than those ionizing the bulk of the nebula.

Both the eastern and western sources require ionizing radiation characterized by a spectral type ~O5.5. One O5.5 V star could ionize the western source, whereas ~three such stars are required by the eastern source. The Lyman continuum luminosity derived from the fine-structure line fluxes is ~one-third that derived from the radio continuum. This may result from diffuse emission outside of the region mapped or a underestimate of the extinction to the nebula. The infrared continuum emission from G298.2 is at least twice that which can be explained by Lyα heating, suggesting, as with the other sources observed, direct stellar heating of the dust.

e) *G29.9+0.0*

G29.9+0.0 (Fig. 8) has been observed by Soifer and Pipher (1975), who detected Ne II and Ar III and by Lester (1979) who detected Ne II, Ar III, and S IV. Lester observed a Ne II flux of 2.7×10^{-10} ergs s^{-1} cm^{-2}, an Ar III flux of 2.7×10^{-11} ergs s^{-1} cm^{-2}, and a S IV flux of 9.3×10^{-12} ergs s^{-1} cm^{-2} in a 3.4″×6.8″ beam. Soifer and Pipher observed a Ne II flux of 8.8×10^{-10} ergs s^{-1} cm^{-2} and an Ar III flux of 8.8×10^{-11} ergs s^{-1} cm^{-2} in a 22″ beam, and we observed a Ne II flux of 8.4×10^{-10} ergs s^{-1} cm^{-2} on a map showing the object to extend out to a diameter of ~30″. The Ar III and S IV results of Lester, scaled by the ratio of his Ne II flux to ours, are given in Table 2 and used in the discussion below.

The Lyman continuum luminosity of G29.9 derived from the fine-structure line fluxes is about twice that derived from radio observations, indicating an overestimate of the extinction or an overabundance of metals, specifically neon. Since a moderate overabundance of neon would be required even with no extinction correction, the results for this nebula, at a galactic radius of ~5 kpc, suggest the presence of a galactic abundance gradient. This conclusion has also been reached by Herter *et al.* (1980).

The fine-structure line intensity ratios indicate that G29.9 is ionized by an O8.5 spectrum. About five O8.5 V stars would provide the ionizing luminosity inferred from the radio flux. In this respect, G29.9 resembles but is less extreme than G333.6−0.2 which is a centrally concentrated symmetric nebula appearing to require many rather cool ionizing stars to explain its ionization (Rank *et al.* 1978; Greenberg 1978). In both cases the excitation is rather uniform across the nebula, arguing against the presence of a hot central star whose spectrum is softened by dust in the nebula. The central peak of G333.6 has been found to break up into several condensations at high spatial resolution (Roche and Aitken 1980; Geballe *et al.* 1981), supporting the suggestion of multiple ionizing stars. As with all of the nebulae discussed in this paper, except W3, the 2–20 μm luminosity cannot be explained solely by Lyα heating. In this case, the relatively constant excitation across the nebula indicates that if dust absorbs starlight directly, it does not do so selectively.

VI. SUMMARY AND DISCUSSION

a) *Morphology*

The five H II regions discussed in this paper were selected for high surface brightness on the basis of radio continuum, infrared continuum, or previous infrared line observations. Because of this selection, all sources are either young, compact nebulae or dense cores of very luminous sources. Surprisingly, a very diverse collection of structures was found.

W3A and B appear to be isolated H II regions in a relatively uniform part of a molecular cloud. Each prob-

© American Astronomical Society • Provided by the NASA Astrophysics Data System

1982ApJ...255..510L

ably has one dominant ionizing star, although a secondary star has been seen in W3A. If these H II regions formed near the edge of a molecular cloud, they have not yet broken out of it. Both show shell structure, but little large scale clumping within the ionized gas. The shell structure probably results from radiation pressure or stellar winds.

The large scale structure of NGC 3576 fits that expected in the sequential star formation model of Elmegreen and Lada (1977). The ionized gas observed in the infrared results from the most recent generation of star formation; an older H II region is seen optically just to the east. There is evidence that the younger H II region is now breaking out of the molecular cloud into the diffuse region. A remarkable degree of clumping is seen which appears to be unrelated to the distribution of ionizing stars. It probably results from clumping which was present in the molecular cloud before it was ionized. No evidence of shadowing by the clumps is seen, suggesting that they are largely optically thin to the ionizing radiation, although their cores must be quite dense if the clumps are to be replenished from neutral condensations, as seems necessary to explain their lifetimes.

The part of NGC 3603 observed is the dense core of a much larger giant H II region. It may be the last remnant of a molecular cloud which is being ionized by a young star cluster. Like NGC 3576, NGC 3603 is remarkably clumpy. In this case shadowing is evident, with S IV emission displaced toward the star cluster from the Ne II emission.

G298.2−0.3 is too distant to allow a detailed study of its structure. Radio observations show a core-halo morphology like NGC 3603.

G29.9+0.0 is a symmetric nebula like W3A and B, but is centrally peaked, not shell-like. Its structure (and excitation) is very similar to that of G333.6−0.2, which has been described as a face-on, blister type source (Hyland *et al.* 1980).

The most striking aspect of the structure of these H II regions is their diversity. Except for NGC 3603 and G298.2, both of which appear to be dense cores of giant H II regions, each of the sources seems to require a different model to explain its structure. Different ages of the H II regions and conditions in the parent molecular clouds may explain the diversity of structures seen. Many of the nebulae show substantial clumping. Clumps which were present in a molecular cloud can be expected to cause nonuniform emission for some period of time early in the life of an H II region. However, once the clumps are entirely ionized they will expand at ~ 10 km s^{-1}, disappearing in $\lesssim 10^4$ yr. Clumps might persist for longer times if they could be replenished from neutral cores, or if new condensations could form. Neutral condensations could result from flows out of a molecular cloud or condensations in a molecular cloud which are enveloped as the H II region expands. For example, NGC 3576 and NGC 3603 both show considerable clumping on scales of 0.1–0.5 pc, although their large scale structures and probably their ages are quite different. Since NGC 3576 appears to be a young H II region embedded in a molecular cloud, its clumpy structure could result from neutral condensations remaining from its birth or from flows out of the surrounding molecular cloud. For dense condensations to remain after the formation of a star cluster and ionization of a giant H II region in the case of NGC 3603, they must have been present as very dense condensations in a molecular cloud which has now nearly dispersed.

b) *Excitation*

In terms of the number of exciting stars present, W3 is the simplest nebula studied. One star probably dominates the ionization of each source. The luminosity of the nebula is somewhat higher than expected for a main-sequence star of the inferred spectral type, but the discrepancy is not large.

NGC 3576 requires a small number of ionizing stars, possibly only two. If the excitation is in fact dominated by only two stars of the inferred spectral types, there would be a problem providing enough ionizing luminosity in this case as well. The most extreme discrepancy between inferred spectral type and luminosity is G29.9 which appears to require at least five O8.5 V stars.

The cores of the two giant H II regions, G298.2 and NGC 3603, are ionized by clusters of rather hot stars. In each case, the observed gas can be ionized by only a few stars, but the halo observed at radio wavelengths requires much more luminosity.

A nearly universal problem in these as well as other compact H II regions is that they appear to require a larger ionizing luminosity than that provided by a main-sequence star of the appropriate spectral type. Several explanations for this problem have been suggested here and elsewhere. (1) OB associations could form which are dominated by several similar stars rather than one very luminous member. This situation has been suggested for G29.9, G333.6, and Sgr A West (Lacy *et al.* 1980). (2) The young stars which ionize compact H II regions could lie above the main sequence. (3) The spectra of luminous, hot stars could be softened by absorption by dust in H II regions if the dust were to preferentially absorb the harder ultraviolet radiation. This third suggestion seems promising for W3 and NGC 3603, where Ne II emission is found farther from the ionizing stars than S IV, but cannot easily explain G333.6 or G29.9, which have uniformly low excitation. A fourth explanation is suggested by the discussion of model uncertainties in § IV. Although we have used Balick and Sneden's (1976) model nebulae with $n_e = 10^3$ cm^{-3}, the models calculated by Köppen (private communication) would require a substantially hotter star for a given

© American Astronomical Society • Provided by the NASA Astrophysics Data System

1982ApJ...255..510L

excitation. In contrast, Stasinska's (1978) models would require much cooler stars. If Köppen's models, which use Kurucz, Peytreman, and Avrett's (1974) model stellar spectra, are the more accurate, hotter and therefore more luminous stars than those discussed here are probably present. Most of the observed nebulae could then be ionized by only one or two dominant ionizing stars. Stasinska's model nebulae, using Mihalas's (1972) stellar spectra, appear to be ruled out by the very large predicted $x(S^{+3})/x(Ne^{+})$ ratios.

A second problem found in this study of excitation of H II regions is that the infrared luminosity of the observed nebulae is almost always larger than can be explained by Lyα heating. Absorption of ionizing or nonionizing stellar radiation by dust is the most likely cause of this phenomenon. This absorption may or may not soften the ionizing radiation, depending on the absorption spectrum of the dust.

We are very grateful for the contributions made to this project by several people. F. Baas and R. J. Brucato built instrumentation for these observations and assisted in the observations, R. H. Rubin and J. Köppen provided calculations of model nebulae and helpful discussions, B. Balick and T. R. Gull supplied the photographs of NGC 3576 and NGC 3603 in Figures 4 and 6, and C. H. Townes provided advice and encouragement throughout this project. We also thank the staffs of Las Campanas and Lick observatories for their assistance. This work was supported by grants from the NSF and NASA.

REFERENCES

Allen, C. W. 1973, *Astrophysical Quantities* (London: Athlone).
Balick, B., Boeshaar, G. O., and Gull, T. R. 1980, *Ap. J.*, **242**, 584.
Balick, B., and Sneden, C. 1976, *Ap. J.*, **208**, 336.
Beck, S. C., Lacy, J. H., Townes, C. H., Aller, L. H., Geballe, T. R., and Baas, F. 1981, *Ap. J.*, **249**, 592.
Becklin, E. E., Matthews, K., Neugebauer, G., and Willner, S. P. 1978, *Ap. J.*, **220**, 831.
Beetz, M., Elsässer, H., and Weinberger, R. 1974, *Astr. Ap.*, **34**, 335.
Brocklehurst, M. 1972, *M.N.R.A.S.*, **160**, 198.
Colley, D. 1980, *M.N.R.A.S.*, **193**, 495.
Elmgreen, B. G., and Lada, C. J. 1977, *Ap J.*, **214**, 725.
Felli, M., Tofani, G., and D'Addario, R. 1974, *Astr. Ap.*, **31**, 431.
Frogel, J. A., and Persson, S. E. 1974, *Ap. J.*, **192**, 35.
Frogel, J. A., Persson, S. E., and Aaronson, M. 1977, *Ap. J.*, **213**, 723.
Geballe, T. R., Wamsteker, W., Danks, A. C., Lacy, J. H., and Beck, S. C. 1981, *Ap. J.*, **247**, 130.
Gillett, F. C., Forrest, W. J., Merrill, K. M., Capps, R. W., and Soifer, B. T. 1975, *Ap. J.*, **200**, 609.
Greenberg, L. T. 1978, Ph.D. thesis, University of California, Berkeley.
Hackwell, J. A., Gehrz, R. D., Smith, J. R., and Briotta, D. A. 1978, *Ap. J.*, **221**, 797.
Harris, S., and Wynn-Williams, C. G. 1976, *M.N.R.A.S.*, **174**, 649.
Herter, T., *et al.* 1980*a*, preprint.
Herter, T., Pipher, J. L., Helfer, H. L., Willner, S. P., Puetter, R. C., Rudy, R. J., and Soifer, B. T. 1980*b*, preprint.
Hyland, A. R., McGregor, P. J., Robinson, G., Thomas, J. A., Becklin, E. E., Gatley, I., and Werner, M. W. 1980, *Ap. J.*, **241**, 709.
Köppen, J. 1978, *Astr. Ap. Suppl.*, **35**, 111.
______. 1979, *Astr. Ap.*, **80**, 42.
______. 1980, *Astr. Ap. Suppl.*, **39**, 77.
Krueger, T., and Czyzak, S. J. 1970, *Proc. Roy. Soc. London, A*, **318**, 531.
Kurucz, R. L., Peytreman, E., and Avrett, E. H. 1974, *Blanketed Model Atmospheres for Early-Type Stars* (Washington: Smithsonian Institution Press).
Lacasse, M. G., Herter, T., Krassner, J., Helfer, H. C., and Pipher, J. L. 1980, preprint.
Lacy, J. H. 1979, Ph.D. thesis, University of California, Berkeley.
______. 1980, in *IAU Symposium 96, Infrared Astronomy*, ed. C. G. Wynn-Williams and D. P. Cruikshank (Dordrecht: Reidel), p. 237.
Lacy, J. H., Townes, C. H., Geballe, T. R., and Hollenbach, D. J. 1980, *Ap. J.*, **241**, 132.
Lester, D. F. 1979, Ph.D. thesis, University of California, Santa Cruz.
Mihalas, D. 1972, *Non-LTE Model Atmospheres for B and O Stars*, NCAR-TN/STR-76.
Osterbrock, D. E. 1974, *Astrophysics of Gaseous Nebulae* (San Francisco: Freeman).
Panagia, N. 1973, *A.J.*, **78**, 929.
Persson, E. E., Frogel, J. A., and Aaronson, M. 1976, *Ap. J.*, **208**, 753.
Petrosian, V. 1970, *Ap. J.*, **159**, 833.
Rank, D. M., Dinerstein, H. L., Lester, D. F., Bregman, J. D., Aitken, D. K., and Jones, B. 1978, *M.N.R.A.S.*, **185**, 179.
Reifenstein, E. C., Wilson, T. L., Burke, B. F., Mezger, P. G., and Altenhoff, W. J. 1970, *Astr. Ap.*, **4**, 357.
Retallack, D. S., and Goss, W. M. 1975, *M.N.R.A.S.*, **193**, 261.
Roche, P. and Aitken, D. K. 1980, unpublished.
Rohlfs, K. 1974, *Astr. Ap.*, **35**, 177.
Seaton, M. J. 1975, *M.N.R.A.S.*, **170**, 475.
Shaver, P. A., and Goss, W. M. 1970, *Australian J. Phys.*, *Ap. Suppl.*, **14**, 133.
Soifer, B. T., and Pipher, J. L. 1975, *Ap. J.*, **199**, 663.
Stasinska, G. 1978, *Astr. Ap. Suppl.*, **32**, 429.
Willner, S. P. 1977, *Ap. J.*, **214**, 706.
Wilson, T. L., Mezger, P. G., Gardner, F. F., and Milne, D. K. 1970, *Astr. Ap.*, **6**, 364.
Wynn-Williams, C. G., Becklin, E. E., and Neugebauer, G. 1972, *M.N.R.A.S.*, **160**, 1.

S. Ć. BECK: Astronomy Department, Space Sciences Building, Cornell University, Ithaca, NY 14853

T. R. GEBALLE: United Kingdom Infrared Telescope, 900 Leilani St., Hilo, HI 96720

J. H. LACY: Downs Laboratory, 320-47, California Institute of Technology, Pasadena, CA 91125

© American Astronomical Society • Provided by the NASA Astrophysics Data System

1982ApJ...255..510L

FIG. 4.—Ne II line map of NGC 3576 superposed on [S II] photograph taken by T. R. Gull

LACY *et al.* (*see* page 516)

© American Astronomical Society • Provided by the NASA Astrophysics Data System

1982ApJ...255..510L

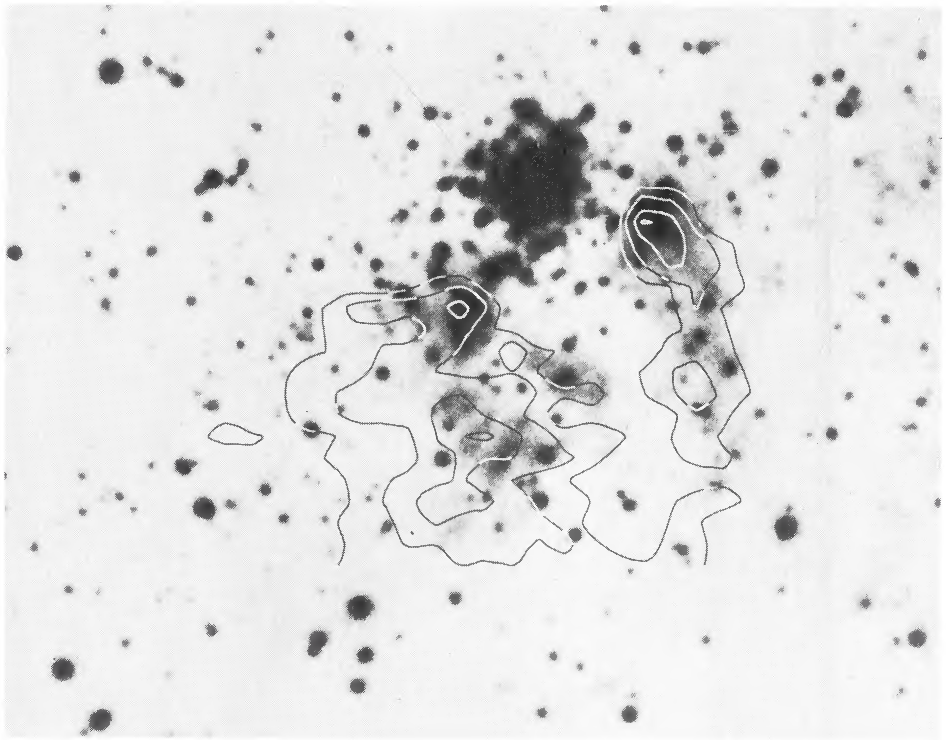

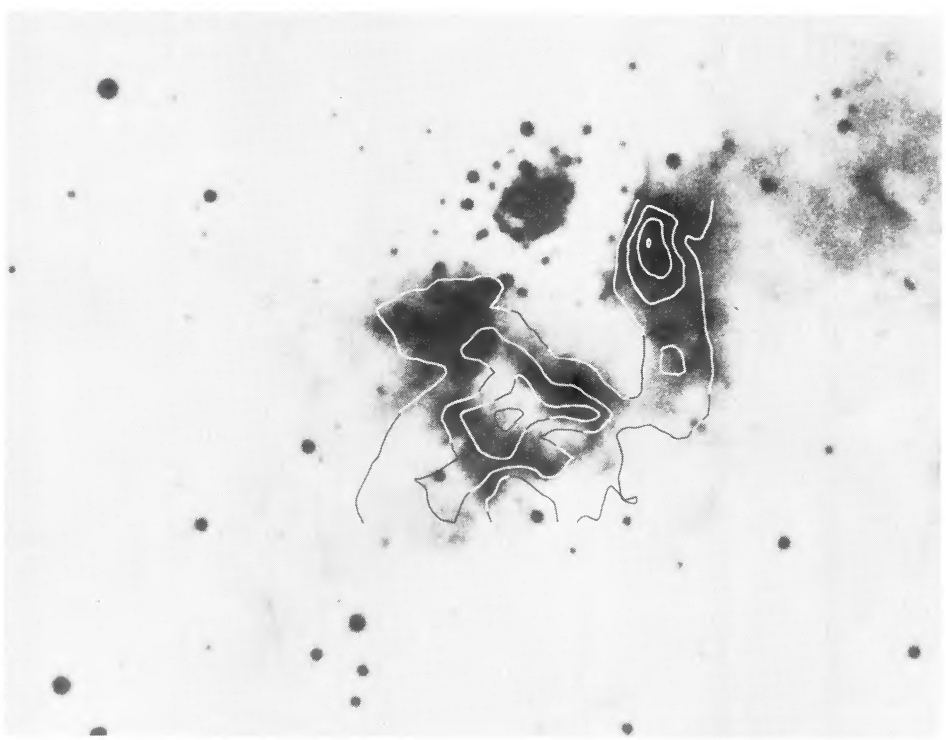

FIG. 6.—Ne II line map of NGC 3603 superposed on [S II] photograph (*upper*) and S IV map superposed on [O III] photograph (*lower*). Photographs were taken from Balick, Boeshaar, and Gull (1980).

LACY *et al.* (*see* page 518)

© American Astronomical Society • Provided by the NASA Astrophysics Data System